bioRxiv preprint doi: https://doi.org/10.1101/531335; this version posted January 26, 2019. The copyright holder for this preprint (which was not certified by peer review) is the author/funder, who has granted bioRxiv a license to display the preprint in perpetuity. It is made available under aCC-BY-NC-ND 4.0 International license.

Comparative Transcriptomic Signature of the Simulated Microgravity Response in *Caenorhabditis elegans*

İrem Çelen[a,b], Aroshan Jayasinghe[b] , Jung H. Doh[b], and Chandran R. Sabanayagam[b,1]

[a]Center for Bioinformatics and Computational Biology, University of Delaware, Newark, DE, USA, 19711

[b]Delaware Biotechnology Institute, University of Delaware, Newark, DE, USA, 19711

[1]Corresponding author:
Chandran R. Sabanayagam
Delaware Biotechnology Institute
University of Delaware
15 Innovation Way, Newark, DE 19711
Telephone: (302) 831-1691
E-mail: chandran@udel.edu

Contact information of the authors:

İrem Çelen: irem@udel.edu
Aroshan Jayasinghe: aroshan@udel.edu
Jung H. Doh: jdoh@udel.edu
Chandran R. Sabanayagam: chandran@udel.edu

bioRxiv preprint doi: https://doi.org/10.1101/531335; this version posted January 26, 2019. The copyright holder for this preprint (which was not certified by peer review) is the author/funder, who has granted bioRxiv a license to display the preprint in perpetuity. It is made available under aCC-BY-NC-ND 4.0 International license.

Keywords: Ceramide, sphinogolipid signaling, longevity, transcriptome, space, intergenerational, microgravity

Abstract

Background

Given the growing interest in human exploration of space, it is crucial to identify the effect of space conditions on biological processes. The International Space Station (ISS) greatly helps researchers determine these effects. However, the impact of the ISS-introduced potential confounders (e.g., the combination of radiation and microgravity exposures) on the biological processes are often neglected, and separate investigations are needed to uncover the impact of individual conditions.

Results

Here, we analyze the transcriptomic response of *Caenorhabditis elegans* to simulated microgravity and observe the maintained transcriptomic response after return to ground conditions for four, eight, and twelve days. Through the integration of our data with those in NASA GeneLab, we identify the gravitome, which we define as microgravity-responsive transcriptomic signatures. We show that 75% of the simulated microgravity-induced changes on gene expression persist after return to ground conditions for four days while most of these changes are reverted after twelve days return to ground conditions. Our results from integrative RNA-seq and mass spectrometry analyses suggest that simulated microgravity affects longevity regulating insulin/IGF-1 and sphingolipid signaling pathways.

Conclusions

Our results address the sole impact of simulated microgravity on transcriptome by controlling for the other space-introduced conditions and utilizing RNA-seq. Using an integrative approach, we

bioRxiv preprint doi: https://doi.org/10.1101/531335; this version posted January 26, 2019. The copyright holder for this preprint (which was not certified by peer review) is the author/funder, who has granted bioRxiv a license to display the preprint in perpetuity. It is made available under aCC-BY-NC-ND 4.0 International license.

identify a conserved transcriptomic signature to microgravity and its sustained impact after return to the ground. Moreover, we present the effect of simulated microgravity on distinct ceramide profiles. Overall, this work can provide insights into the sole effect of microgravity on biological systems.

Background

Significant efforts have being made for the exploration of space. As such, NASA and SpaceX have planned round-trip landings by 2030s and placement of a million people in 40 years to Mars. However, space conditions present different types of environmental stress such as increased levels of radiation and reduced gravity (i.e., microgravity) that negatively affect biological processes by causing changes in the transcriptome leading to bone loss, muscle atrophy, and immune system impairment, to name a few examples. To overcome this problem, the affected biological mechanisms in space conditions should be uncovered to take precautions before the colonization of Mars.

The International Space Station (ISS) has provided a great opportunity to study the impact of space conditions on biological systems. However, potential confounders at the ISS are generally neglected. For example, experiments in the ISS introduces elevated radiation and reduced gravity along with the hypergravity during the launch. These mixed stress factors make it highly challenging to detect what precisely causes the observed phenotypes. To identify how the space conditions affect the biological systems, each of the factors require a separate investigation.

Microgravity is one of the major stress factors causing detrimental health effects on humans. Simulation of microgravity is a cost-effective way to study the impact of microgravity

bioRxiv preprint doi: https://doi.org/10.1101/531335; this version posted January 26, 2019. The copyright holder for this preprint (which was not certified by peer review) is the author/funder, who has granted bioRxiv a license to display the preprint in perpetuity. It is made available under aCC-BY-NC-ND 4.0 International license.

on biological systems. For this purpose, various platforms including drop towers, parabolic flights and space flights are available. Because of their advantages to enable long term simulations in an effective and economical manner, clinostats are widely preferred to study gravitational response in biological systems, mainly plants, for decades [1–5]. Clinostats rotate a sample around a horizontal axis, thereby exposing the sample to a rotating gravitational vector. This can reduce and even possibly remove gravitational bias in the development of an organism [3, 6–10].

C. elegans is an ideal model organism for space biology studies with its completely documented cell lineage, high reproduction rate, short lifespan, and high similarity to the human genome [11–16]. In the public bioinformatics repository of NASA (GeneLab; https://genelab.nasa.gov), four studies from three missions to the International Space Station (ISS) are available from *C. elegans* (Table 1). However, the experimental design of these studies highly varies. For example, these studies adopted different food source (e.g., axenic or monoxenic liquid media), duration of study, developmental stage, or the worm strain while the usage of microarray technology was common for all. We and others have reported substantial variations in the transcriptomic and phenotypical responses to different liquid cultivations of the worms [11, 17]. We additionally showed that two strains of *C. elegans* (N2 and AB1) exhibit highly different transcriptomic profiles under liquid cultivations [11, 16]. Overall inconsistency among the space biology experiments on *C. elegans* highlights the necessity of a more organized and uniform experimental design for future studies where each stress factor is investigated individually.

This study investigates the sole effect of simulated microgravity on *C. elegans* transcriptome and the sustained impacts after return to ground control conditions. We report a

bioRxiv preprint doi: https://doi.org/10.1101/531335; this version posted January 26, 2019. The copyright holder for this preprint (which was not certified by peer review) is the author/funder, who has granted bioRxiv a license to display the preprint in perpetuity. It is made available under aCC-BY-NC-ND 4.0 International license.

group of putative microgravity-responsive genes, we define as the gravitome, through the integration of our in-house data with the re-analyzed *C. elegans* data from GeneLab. Through the RNA-sequencing (RNA-seq) and mass spectrometry analyses, we reveal the downregulation of the sphingolipid signaling pathway and its potential function in longevity under simulated microgravity.

Table 1. An overview of the *C. elegans* studies at the ISS. PRJNA146465 represents the study conducted by Universiti Kebangsaan Malaysia (UKM).

	Food Source	Duration	Strain	Develop. Stage	Technology	Year
ICE-First	CeMM	10 days	N2	Mixed	Microarray	2004
PRJNA146465	CeMM	6 months	CC1	Mixed	Microarray	2006
CERISE-4	S-Medium	4 days	N2	~L4	Microarray	2009
CERISE-8	S-Medium	8 days	N2	Mixed	Microarray	2009

Results

To dissect the biological processes affected under simulated microgravity and sustained after the exposure, we first cultured *C. elegans* in CeHR for three weeks on ground control condition. Then, we exposed the worms to clinostat-simulated microgravity for four days (Fig. 1a; Additional file 2: Movie S1) and observed the maintained impacts at four, eight, and twelve days after placing the worms back to ground conditions (Fig. 1b). RNA-seq was performed for each condition with three replicates (Additional file 3: Dataset S1). Because RNA-seq can detect

bioRxiv preprint doi: https://doi.org/10.1101/531335; this version posted January 26, 2019. The copyright holder for this preprint (which was not certified by peer review) is the author/funder, who has granted bioRxiv a license to display the preprint in perpetuity. It is made available under aCC-BY-NC-ND 4.0 International license.

low abundance transcripts and achieve less noise in the data, unlike previous space biology studies on *C. elegans*, we preferred RNA-seq over microarray [18].

We generated a dendrogram for the transcriptomic profile in each condition tested and found significant differences during and after exposure to simulate microgravity compared to the ground control conditions (Fig. 1c). Thus, this result suggests that exposure to simulated gravity induces highly distinct gene expression patterns which are maintained even after 12 days return to ground conditions (approximately three generations of *C. elegans* in axenic medium [19]).

Simulated microgravity triggers differential expression of hundreds of genes

To identify the genes with the most distinctive expression levels after the exposure, we determined the differentially expressed genes (DEGs). The genes with over two-fold $\log_2$ expression difference with the FDR-adjusted *p-value* ≤ 0.05 were considered as DEGs. Hundreds of genes demonstrated differential expression during exposure to simulated microgravity and up to eight days after return to ground conditions (Fig. 1d). Twelve days after the return, the gene expression levels started to resemble the ones in the ground control with only 91 upregulated and 13 downregulated genes.

The determination of the spatial expression of the DEGs is of great importance to identify the potentially affected tissues. Thus, we performed tissue enrichment analysis for the DEGs in simulated microgravity (Fig. 2a). The downregulated genes were overrepresented in neuronal and epithelial tissues, and intestine while the upregulated genes were enriched in the reproductive system-related tissues.

Next, we conducted pathway enrichment analysis for the DEGs in simulated microgravity and return to ground conditions to identify the altered pathways and whether they are remained

bioRxiv preprint doi: https://doi.org/10.1101/531335; this version posted January 26, 2019. The copyright holder for this preprint (which was not certified by peer review) is the author/funder, who has granted bioRxiv a license to display the preprint in perpetuity. It is made available under aCC-BY-NC-ND 4.0 International license.

to be altered after return to ground conditions (Fig. 2b). Our results suggested an upregulation of dorso-ventral axis formation and downregulation of lysosome during the exposure, and these expression patterns were maintained for four and eight days after the return, respectively.

Simulated microgravity-induced gene expression differences are highly maintained for eight days after return to ground conditions

We then identified the number of simulated microgravity-induced DEGs that preserved their expression patterns after the return (Fig. 2c). The majority of the DEGs (approximately 75%) from the exposed animals maintained their expression patterns after the return for four days. The shared number of DEGs decreased drastically at 12 days after the return to 16% for commonly upregulated and <1% downregulated genes with the exposed animals.

To elucidate the genes showing altered expression under simulated microgravity and maintaining these expression patterns after return to ground conditions for short (4 days) and long-term (12 days), we categorized the DEGs in Venn diagrams (Fig. 2d, e; Additional file 4: Dataset 2). The genes solely upregulated in the exposed animals did not exhibit enrichment for any gene ontology (GO) term. The genes upregulated during the exposure and four days after the return, however, showed an overrepresentation for reproduction-related processes (Fig. 2d). Chitin metabolic process-related genes were induced at four days after return to ground conditions, and the expression profiles were conserved for eight days after the return.

We found that the downregulated genes were enriched for the biological processes which are affected in space conditions. In particular, genes functioning in body morphology, collagen and cuticulin-based cuticle development, defense response, and locomotion were downregulated under simulated microgravity and up to eight days after return to ground conditions (Fig. 2e). In simulated microgravity and spaceflight studies, both small movement defects [20] and no

bioRxiv preprint doi: https://doi.org/10.1101/531335; this version posted January 26, 2019. The copyright holder for this preprint (which was not certified by peer review) is the author/funder, who has granted bioRxiv a license to display the preprint in perpetuity. It is made available under aCC-BY-NC-ND 4.0 International license.

difference in locomotory behavior [21, 22] have been noted. The reason behind these discrepancies is unclear, but our results indicated differences in the expression of the locomotion genes in close to weightless environment. Similarly, neuropeptide signaling pathway genes (*flp-22*, *flp-8*, *flp-26*, *nlp-10*, *nlp-12*, *nlp-17*, *nlp-20*, *nlp-24*, *nlp-25*, *nlp-26*, *nlp-39*, *nlp-33*, *nlp-28*, *nlp-29*, *nlp-30*, and *flp-24*) were downregulated during the exposure, and this expression profile was lost after return to ground conditions (Fig. 2e). These neuropeptide signaling pathway genes also exhibit enrichment for movement variant phenotypes (Additional File 1: Fig. S1) indicating altered locomotion in response to simulated microgravity.

During the spaceflight, the neuromuscular system and collagen have been negatively affected [20]. In agreement with these findings, collagen genes were downregulated in our experiment during the exposure, and the downregulation was sustained for eight days after return to ground conditions. Previously, Higashibata et al. (2006) reported decreased expression for the myogenic transcription factors and myosin heavy chains in space-flown worms [20]. We did not observe differential expression for these muscle-related genes. Since their reported flight to ground gene expression ratio for the downregulated genes was less than one, and we only consider the genes with the log2 ratio greater than two as DEG, it is expected not to observe those genes in our group of DEGs. To test whether other muscle-related genes are differentially expressed under simulated microgravity, we compared our DEGs to 287 genes reported in WormBase for involvement in muscle system morphology variant or any of its transitive descendant terms via RNAi or variation. Only T14A8.2, *col-103*, and *sqt-3* among the 287 genes showed downregulation under simulated microgravity (hypergeometric test, *p-value* = 0.99). Thus, our results did not suggest a significant change in the expression of the genes known to function in muscle morphology.

bioRxiv preprint doi: https://doi.org/10.1101/531335; this version posted January 26, 2019. The copyright holder for this preprint (which was not certified by peer review) is the author/funder, who has granted bioRxiv a license to display the preprint in perpetuity. It is made available under aCC-BY-NC-ND 4.0 International license.

In our previous work, we revealed that the expression of many ncRNA molecules is triggered in response to environmental changes [16]. To identify whether a similar pattern occurs under simulated microgravity, we determined the expressed ncRNA molecules in ground control, simulated microgravity, and return. Since the housekeeping gene *pmp-3* presents consistent expression patterns [16], we considered its minimum expression level (FPKM = 24.7) in our experiment as the cutoff for the expression of ncRNA molecules. The number of expressed ncRNA molecules slightly decreased in response to simulated microgravity (Additional file 1: Fig. S2a). Interestingly, this number increased drastically in the eighth day of return. We found that the expression of 126 ncRNA molecules is induced in simulated microgravity and for 12 days after the return (Additional file 1: Fig. S2b) while the expression of 16 ncRNA molecules is lost during and after simulated microgravity (Additional file 1: Fig. S2c). Among the classified ncRNA molecules, mostly snoRNA and lincRNA molecules are induced while other sets of snoRNA and asRNA molecules lose expression in simulated microgravity. For instance, asRNA molecules *anr-33*, K12G11.14, and ZK822.8 are induced whereas *anr-2*, *anr-9*, and Y49A3A.6 are silenced during and 12 days after the exposure.

We next sought to identify the putative transcriptional regulators (i.e., transcription factors) of the simulated microgravity-induced genes and whether these regulators maintain their impact after return to ground conditions. That is, we determined the putative transcription factor (TF) genes [23] that are upregulated under simulated microgravity and after the return. Our results have revealed that 20 TF genes are upregulated during the exposure and 90%, 75%, and 15% of these genes maintained their upregulation after the return for four, eight, and twelve days, respectively (Additional File 1: Fig. S3). These TFs play a role in a variety of mechanisms such as double strain break repair or sex determination. For example, *tbx-43* is upregulated

bioRxiv preprint doi: https://doi.org/10.1101/531335; this version posted January 26, 2019. The copyright holder for this preprint (which was not certified by peer review) is the author/funder, who has granted bioRxiv a license to display the preprint in perpetuity. It is made available under aCC-BY-NC-ND 4.0 International license.

during the exposure and for at least 12 days after the return. The best human BLASTP-match of *tbx-43* in WormBase, TBR, functions in developmental process and is required for normal brain development (E-value = 3e-33; identity = 68.5%). However, many of the upregulated TFs do not have a known function. Hence, our list of simulated microgravity-induced TF gene expressions can be a rich source for the discovery of the microgravity-related transcriptional regulators.

Longevity regulating pathways are affected under simulated microgravity

Spaceflight affects the mechanisms involved in delayed aging in worms. For instance, Honda et al. found that age-dependent increase of 35-glutamine repeat aggregation is suppressed and seven longevity-controlling genes are differentially expressed in spaceflight [24, 25]. To examine whether simulated microgravity induces such changes, we mapped the DEGs to longevity regulating pathway in the Kyoto Encyclopedia of Genes and Genomes (KEGG). We used a less stringent criterion for differential expression by including the genes with $\log_2$(FPKM) > 1.5 in this analysis. We determined 11 DEGs in the longevity regulating pathway genes most of which are involved in the insulin/insulin-like growth factor signaling pathway (insulin/IGF-1)(Fig. 3). Interestingly, the transcription factor DAF-16 gene did not exhibit differential expression unlike its targets *sod-3*, *lips-17*, and *ctl-1*. Because the translocation of DAF-16 into the nucleus activates or represses target genes functioning in longevity, metabolism, and stress response, this finding was unexpected [26–29]. The nuclear localization of DAF-16 is antagonized by transcription factor PQM-1 [30], and thus an upregulation in *pqm-1* may indicate inhibition of DAF-16 translocation. Our data, however, did not present a differential expression for *pqm-1* and thus it does not suggest inhibition of the DAF-16 translocation. It is possible that the DAF-16 targets are differentially expressed due to translocation state of DAF-16 or involvement of other factors (e.g., other transcriptional regulators).

bioRxiv preprint doi: https://doi.org/10.1101/531335; this version posted January 26, 2019. The copyright holder for this preprint (which was not certified by peer review) is the author/funder, who has granted bioRxiv a license to display the preprint in perpetuity. It is made available under aCC-BY-NC-ND 4.0 International license.

The upregulation of the longevity regulating pathway transcriptional targets generally contributes to increased lifespan. Since many of these targets were downregulated under simulated microgravity, we wished to identify the potential impact of their downregulation by acquiring their RNAi phenotype from WormBase [31]. Lifespan variant (WBRNAi00063155 and WBRNAi00063156) for *hsp-12.6* and extended lifespan (WBRNAi00064044) for *sod-3* have been reported. Follow-up experiments are needed to fully understand the role of these genes in the longevity regulation under simulated microgravity.

To further investigate the involvement of the longevity genes in simulated microgravity, we compared the DEGs to the DAF-16-responsive genes [30]. We found 144 DAF-16-induced genes were downregulated and this overlap was statistically significant (hypergeometric test, *p-value* < 0.0001). The number of shared genes between the simulated microgravity-induced genes and the genes induced or repressed by DAF-16 are 11 and 35, respectively (hypergeometric test, p-value > 0.05 for both). Similarly, the number of downregulated DAF-16-repressed genes were insignificant with a total of 57 shared genes (hypergeometric test, p-value > 0.05) (Additional File 5: Dataset S3). Together, our results suggest that the longevity regulation genes are affected under simulated microgravity and that along with the DAF-16-regulation, other mechanisms have an important function in this process.

Sphingolipid signaling pathway is suppressed in response to simulated microgravity

Previous studies have suggested that the sphingolipid signaling pathway plays a role in the expression of DAF-16/FOXO-regulated genes [32, 33]. In line with this, our results showed that the sphingolipid signaling pathway is downregulated under simulated microgravity. That is, putative glucosylceramidase 4 gene (*gba-4*) and putative sphingomyelin phosphodiesterase *asm-3* are downregulated and these downregulation patterns were sustained for eight days after return

bioRxiv preprint doi: https://doi.org/10.1101/531335; this version posted January 26, 2019. The copyright holder for this preprint (which was not certified by peer review) is the author/funder, who has granted bioRxiv a license to display the preprint in perpetuity. It is made available under aCC-BY-NC-ND 4.0 International license.

to ground conditions (Fig. 4a). This downregulation pattern indicates an attenuation in the ceramide levels through a potential decrease in the degradation of sphingomyelin and glucosylceramide to ceramide. Along with the other biological functions such as autophagy, senescence, and apoptosis, the sphingolipid signaling pathway has critical functions in ageing and longevity regulation [32, 34, 35]. The inhibition of this conserved pathway results in an extension of lifespan in animals from worms to humans [34, 35]. For example, the inactivation of *asm-3* in *C. elegans* causes translocation of DAF-16 into the nucleus, promotion of DAF-16 target gene expression, and extension of lifespan by 14% - 19% [33].

To validate the ceramide and sphingosine levels are indeed decreased in response to the aforementioned gene downregulations, we performed mass spectrometry analysis in ground control and simulated microgravity-exposed worms concurrently (Additional file 6: Dataset S4; Fig. 4b,c). Our results revealed that total ceramide, total hexosylceramide (HexCer), and d18:1 sphingosine are lower (1.5-, 3.6-, and 1.4-fold, respectively) under simulated microgravity (t-test, p-value < 0.05). Similarly, sphingoid base (SB) levels decreased 1.9-fold under simulated microgravity, but this decrease was not significant (t-test, p-value = 0.055) (Fig. 4b). Interestingly, the levels of total lactosylceramide (LacCer) increased by 27-fold (t-test, p-value $<$ 0.05). Increase in the LacCer and HexCer levels have been determined as biomarkers of aging in humans and murine [36] while LacCer C18:1 was unaffected during aging in *C. elegans* [34]. It is unclear why LacCer levels are elevated when the HexCer levels are decreased, but the overall pattern indicates a downregulation in the sphingolipid signaling pathway under simulated microgravity.

The levels of long acyl-chain ceramides ($\geq$C24) are elevated with advancing age and in age-related diseases such as diabetes and cardiovascular disease while C20 and C26 ceramides

bioRxiv preprint doi: https://doi.org/10.1101/531335; this version posted January 26, 2019. The copyright holder for this preprint (which was not certified by peer review) is the author/funder, who has granted bioRxiv a license to display the preprint in perpetuity. It is made available under aCC-BY-NC-ND 4.0 International license.

277 are unaffected with aging or developmental stage in *C. elegans* [34, 37, 38]. To further decipher
278 the potential effect of simulated microgravity on aging-related mechanisms, we quantified the
279 levels of different acyl-chain ceramides (Additional file 6: Dataset S4; Fig. 4c). We observed a
280 decrease in d18:1-C24, and d18:1-C24:1 ceramides (1.2-, and 3.2-fold, respectively) under
281 simulated microgravity (t-test, p-value < 0.05). It has been found that the inhibition of C24-C26
282 ceramide-inducing ceramide synthase HYL-1 causes improvements in neuromuscular function
283 and age-dependent hypoxia and stress response [39, 40]. Hence, the lower levels of C24 and
284 C24:1 ceramides in the simulated microgravity-exposed worms may indicate their positive
285 impact on the stress response and aging of the worms.

286 Along with their roles in aging and longevity, different acyl-chain ceramides have other
287 distinctive functions. For example, C16-ceramide induces germ cell apoptosis [41] and C20-C22
288 ceramide functions in resistance to hypoxia [40]. We determined that ceramides with different
289 acyl-chain showed altered levels in response to simulated microgravity. While d18:1-C16 and
290 d18:1-C18 exhibited a decrease (2.8- and 1.6-fold, respectively), d18:1-C20 and d18:1-C22
291 ceramides exhibited an increase (3.7- and 1.5-fold, respectively) under simulated microgravity (t-
292 test, p-value < 0.05). Collectively, our findings suggest that sphingolipid and insulin/IGF-1
293 pathways play a role in simulated microgravity response.

294 **Identification of the "gravitome" through comparison of the microgravity-exposed worm**
295 **gene expression profiles**

296 To investigate the "gravitome", we compared the results from our simulated microgravity
297 experiment to those from previous spaceflight experiments on *C. elegans* reported in NASA's
298 GeneLab database (https://genelab.nasa.gov/). For this analysis, we used GEO2R to determine
299 the microarray DEGs (|log2 fold change (logFC)| > 2 and adj. *p-value* < 0.05) from the first

bioRxiv preprint doi: https://doi.org/10.1101/531335; this version posted January 26, 2019. The copyright holder for this preprint (which was not certified by peer review) is the author/funder, who has granted bioRxiv a license to display the preprint in perpetuity. It is made available under aCC-BY-NC-ND 4.0 International license.

International *C. elegans* Experiment in Space (ICE-First), *C. elegans* RNA Interference in Space Experiment (CERISE) four and eight days, and PRJNA146465 conducted by UKM. We reasoned that the genes that are commonly differentially expressed in all the studies should be the ones responding to microgravity. Surprisingly, the number of shared DEGs were highly limited among the studies (Fig. 5a). For instance, there were no shared DEGs between ICE-First and the other previous studies, and only five shared DEGs between four and eight days of CERISE. The experimental design of these studies has substantial differences including food source, developmental stage, strain, and exposure time (Table 1). These differences can be the underlying reason causing the highly distinct DEG profiles. For example, in the four-day culture of CERISE, approximately 9,000 L1 worms were used whereas in the eight-day culture, the number of worms was 30 to 50 L1 [42]. Additionally, because the worms become gravid in four days in axenic culture [19, 43], the eight-day culture probably has mixed developmental stage worms as oppose to the synchronized worms in the four-day culture. As expected, the four- and eight-day CERISE cultures showed profound difference in the overall gene expression profiles, as well (Fig. 5b).

Higashibata et al., have reported reproducible gene expressions for myosin, paramyosin, *unc-87*, *dim-1*, sirtuin and its target genes from four-day CERISE and ICE-First [44]. We wished to evaluate the expression of these genes in eight-day CERISE, PRJNA146465, and our study, as well. Additionally, we assessed the expression levels of these genes when a different analysis method (i.e., GEO2R) is used and noted the reported expression levels in different manuscripts for the same studies (Table 2). None of the genes were in our list of DEGs and most of them showed logFC < 1 between the conditions. Furthermore, some genes had high differences in the logFC or discrepancy for up- or downregulation among the experiments. For example, *pqn-5* was

bioRxiv preprint doi: https://doi.org/10.1101/531335; this version posted January 26, 2019. The copyright holder for this preprint (which was not certified by peer review) is the author/funder, who has granted bioRxiv a license to display the preprint in perpetuity. It is made available under aCC-BY-NC-ND 4.0 International license.

323 reported to be 4.18-fold upregulated in the four-day CERISE while it was 0.9-fold
324 downregulated in the ICE-First. The same gene was upregulated 0.25-fold in PRJNA146465
325 (Table 2). These findings highlight the necessity of uniformity in the experimental design and a
326 detailed evaluation of the currently used techniques for achieving more reproducible and
327 accurate results.

328

329

330

331 **Table 2.** Previously reported [44] reproducible gene expression changes from previous
332 spaceflight studies in *C. elegans*. The values represent the logFC of the gene expressions under
333 microgravity versus ground control. NR: not reported, NA: not available.

	CERISE (4 days)		**CERISE (8 days)**	**ICE-First (10 days)**			**UKM (6 months)**		**Simulated Microgravity (4 days)**	
Gene Name	[44]	**GEO2R**	**GEO2R**	[44]	[20]	**GEO2R**	[45]	**GEO2R**	**Cuffdiff2**	**DESeq2**
myo-3	-0.89	-0.78	-0.06	-0.34	-0.30	-0.28	3.12	1.61	-0.18	-0.14
unc-54	-0.49	-0.40	-0.14	-0.45	-0.5	-0.37	NR	-0.47	0.16	0.20
unc-15	-0.62	-0.52	NA	-0.33	-0.2	-0.35	NR	-0.44	0.10	0.15
unc-87	-0.25	-0.30	-0.01	-0.34	NR	-0.29	NR	-0.14	-1.02	-0.98
dim-1	-0.11	-0.39	-0.15	-0.53	NR	-0.34	NR	-0.01	-0.45	-0.41
sir-2.1	0.53	0.59	0.14	0.03*	NR	0.07	NR	0.15	0.56	0.61
abu-7	-1.24	-1.63	-1.18	-0.63	NR	-0.71	NR	-1.05	NA	NA
abu-6	-2.18	-1.91	-1.21	-0.78	NR	-0.72	NR	-0.40	NA	NA
pqn-78	-3.08	-3.11	-1.07	-0.80	NR	-0.73	NR	-0.28	NA	NA
pqn-5	-4.18	-4.89	-1.35	-0.90	NR	-0.41	NR	0.25	NA	NA
lbp-6	-0.47	-0.49	-0.14	-0.61	NR	-0.54	NR	0.43	-1.95	-1.89

334

bioRxiv preprint doi: https://doi.org/10.1101/531335; this version posted January 26, 2019. The copyright holder for this preprint (which was not certified by peer review) is the author/funder, who has granted bioRxiv a license to display the preprint in perpetuity. It is made available under aCC-BY-NC-ND 4.0 International license.

We analyzed our RNA-seq data both with the Tuxedo pipeline [46] and DEseq2 [47] to confirm that the results are not dependent upon the analysis method. The results from both the methods were clustered together indicating their similarity (Fig. 5b). The highest number of DEG overlap was between our experiment and four-day CERISE, and the overlap was significant for both the methods (hypergeometric test, *p-value* < 0.05) (Fig. 5c). Since the overlap between the four-day CERISE and our results from the Tuxedo pipeline is higher, we decided to use the results from this pipeline throughout the manuscript. The results from DEseq2 are reported in the supplementary data (Additional File 1: Fig. S4; Additional File 7: Dataset S5).

We determined a total of 134 common DEGs between our experiment and four-day CERISE, eight of them also being common to PRJNA146465, and categorized these 134 genes as the putative gravitome (Fig. 5a, c; Additional File 8: Dataset S6). We discarded 16 DEGs showing conflicting patterns between the experiments (i.e., upregulated in one experiment and downregulated in the other) for further analyses. We reasoned that if the remaining genes are collaboratively involved in a biologically relevant process, they might have protein-protein interactions (PPIs) with each other. To test this hypothesis, we examined the enrichment for PPI of these genes by using the STRING database [48]. Among 118 DEGs, 58 had known PPIs with each other (FDR < 1.0e-16) indicating their collaborative involvement in a biological process (Fig. 5d). The GO analysis revealed that the gravitome genes play a functional role in locomotion, body morphogenesis, and collagen and cuticulin-based cuticle development (Fig. 5e). Similarly, the gravitome gene products exhibit enrichment for nematode cuticle collagen N-terminal and collagen triple helix repeat domains (Fig. 5f). Together, our findings suggest that mainly the collagen genes are affected under microgravity and this effect is reproducible between the studies.

bioRxiv preprint doi: https://doi.org/10.1101/531335; this version posted January 26, 2019. The copyright holder for this preprint (which was not certified by peer review) is the author/funder, who has granted bioRxiv a license to display the preprint in perpetuity. It is made available under aCC-BY-NC-ND 4.0 International license.

Next, we asked whether the human orthologs of the gravitome genes have relevant functions which might be affected in astronauts. We identified 64 human orthologs to 44 gravitome genes in worms (Additional File 9: Dataset S7). The human orthologs exhibited overrepresentation for protein domains including calpain large subunit domain III and calpain family cysteine protease (Additional file 1: Fig. S5). Given the reported upregulation of calpain under microgravity and its function in muscle atrophy [49, 50], these results provide an additional support for a conserved gravitome in worms and humans.

Our analyses revealed that 20 putative TF genes are upregulated under simulated microgravity conditions. We wondered whether these upregulation patterns are shared in the four-day CERISE. Among the 20 upregulated putative TF genes, Y56A3A.28 and T24C4.2 showed upregulation during the four-day CERISE, indicating a potential transcriptional regulation role for these two in response to microgravity. Our results additionally suggested that the upregulation pattern of these TFs are maintained for eight and twelve days after the return, respectively. We could not find a human ortholog for T24C4.2 while the WormBase-suggested human ortholog of Y56A3A.28 is PRDM16. PRDM16 regulates the switch between skeletal muscle and brown fat cells by inhibiting the skeletal muscle development and gene expression and stimulating brown adipogenesis [51]. Therefore, Y56A3A.28 can be a strong candidate as a negative regulator of the muscle development under microgravity conditions.

Discussion

In this study, we examined the simulated microgravity responsive gene expression patterns and their maintained levels for four, eight, and twelve days after return to ground conditions. Longevity regulating pathways such as insulin/IGF-1 and sphingolipid signaling pathway were affected under simulated microgravity. We identified a putative gravitome by

bioRxiv preprint doi: https://doi.org/10.1101/531335; this version posted January 26, 2019. The copyright holder for this preprint (which was not certified by peer review) is the author/funder, who has granted bioRxiv a license to display the preprint in perpetuity. It is made available under aCC-BY-NC-ND 4.0 International license.

381 determining the common microgravity responsive transcriptomic signatures by incorporating our
382 study to the previous ones. Moreover, we revealed that the gravitome is potentially conserved
383 between worms and humans by performing function analysis for the human orthologs of the
384 worm gravitome and identifying some of their potential transcriptional regulators.

385 Sphingolipid signaling pathway plays crucial biological roles such as lifespan regulation,
386 apoptosis, and oxidative-stress response [32, 34, 52]. Our results revealed an overall
387 downregulation of the sphingolipid pathway which is generally related to an increase in
388 longevity [34]. A recent study identified decreased ASM-1 and ASM-2 levels in the ISS-housed
389 worms indicating a similar downregulation in response to microgravity [53]. Mutant strains or
390 RNAi knockdown of acid sphingomyelinase ASM-1, ASM-2, and ASM-3 genes increase the
391 lifespan, ASM-3 being the most prominent one. Overall, both simulated and the ISS-introduced
392 microgravity seem to contribute to a potential increase in longevity through the downregulation
393 of the sphingolipid signaling pathway. Follow-up experiments are needed to delimitate the
394 contribution of sphingolipids on longevity under microgravity.

395 In the Twins Study of NASA, Scott Kelly was sent to the ISS for 340 days while his
396 identical twin Mark Kelly remained on Earth. The preliminary results from this investigation
397 showed that Scott Kelly's telomere length significantly increased during the mission. The
398 telomere length of Mark Kelly, however, remained relatively stable [54]. Telomere length and
399 lifespan have a strong relationship. That is, longer telomeres are linked to longer lifespan and
400 increased resistance to environmental stress while shorter telomeres are linked to accelerated
401 aging and reduced longevity [55–58]. Ceramide functions in the regulation of telomere length
402 [35, 59]. Considering our findings on decreased ceramide levels and the observations on

bioRxiv preprint doi: https://doi.org/10.1101/531335; this version posted January 26, 2019. The copyright holder for this preprint (which was not certified by peer review) is the author/funder, who has granted bioRxiv a license to display the preprint in perpetuity. It is made available under aCC-BY-NC-ND 4.0 International license.

403 increased telomere in the ISS, investigation of the ceramide and telomere length relationship
404 might prove important to uncover the mechanisms affecting longevity in space.

405 Most of the space flight-triggered physiological changes are reverted after return to Earth
406 [60]. Similarly, we observed that the majority of the simulated microgravity-induced DEGs (over
407 84%) are reverted 12-days after return to ground conditions. Our results have revealed that while
408 some biological processes are only affected during the exposure, others can be affected for at
409 least eight days (approximately two generations) after the return. For example, neuropeptide
410 signaling pathway genes were differentially expressed only during the exposure whereas defense
411 response genes remain downregulated for eight days after the return. Approximately 50% of the
412 astronauts from Apollo mission experienced minor bacterial or viral infections at the first week
413 of their return. Later studies reported that space flight-induced reactivation of latent herpes
414 viruses which lasted for a week after the return to Earth (reviewed in [61]). These consistent
415 observations indicate that the detrimental effects of space conditions (i.e., microgravity) on
416 immune system carry over even after the return. Future investigations could provide insight into
417 whether the duration of the exposure has an impact on the duration of the lasting effects.

418 The limitation of our study is the inclusion of mixed stage worms and the collection of
419 samples from whole animals. This limitation is common among the aforementioned worm
420 experiments conducted in the ISS. Considering the significantly different gene expression
421 patterns among developmental stages and across cell types [62], it is possible to retrieve biased
422 results from the averaged gene expression levels. It is essential to address these issues in future
423 studies.

424 Our integrative approach to define the gravitome has shown that the gene expression
425 profiles widely vary among the experiments. Similarly, the comparison of spaceflight responsive

bioRxiv preprint doi: https://doi.org/10.1101/531335; this version posted January 26, 2019. The copyright holder for this preprint (which was not certified by peer review) is the author/funder, who has granted bioRxiv a license to display the preprint in perpetuity. It is made available under aCC-BY-NC-ND 4.0 International license.

genes in *C. elegans* and *Drosophila melanogaster* demonstrated only six common genes from the European Soyuz flights to the ISS [63]. The reason for these discrepancies can be the batch effects introduced due to the differences in the experimental designs. For instance, different exposure times to the space conditions or the usage of different food source or strain can induce highly distinct responses in the worms. Furthermore, during the missions to the ISS, the organisms experience drastic environmental changes including exposure to radiation, different temperature, and gravitational forces (i.e., hypergravity and microgravity). It is crucial to examine methods used for achieving the most accurate and reproducible results and to identify the effects of individual factors (e.g., diet and gravitational force). Towards that end, we previously reported the impact of liquid cultivation of two *C. elegans* strains on gene expression and phenotype [11, 16] and here, studied the impact of simulated microgravity.

Conclusions

Given the elevated interest in the human exploration of space, it is crucial to determine the detrimental effects of the space conditions on biological systems. Our study demonstrates that *C. elegans* is an efficient model to identify the impact of space on biological systems. We believe that our results will be a valuable reference for the studies on transcriptomic response to microgravity by controlling for the renowned batch effects from space conditions, allowing the worms to acclimate to liquid cultivation before the experiment, presenting the sustained transcriptomic responses after return to ground along with their putative regulators, integrating the results from the previous studies conducted at the ISS, and providing the response of different ceramide profiles to simulated microgravity.

bioRxiv preprint doi: https://doi.org/10.1101/531335; this version posted January 26, 2019. The copyright holder for this preprint (which was not certified by peer review) is the author/funder, who has granted bioRxiv a license to display the preprint in perpetuity. It is made available under aCC-BY-NC-ND 4.0 International license.

Materials and Methods

C. elegans strain and growth conditions

Wild-type N2 strain was obtained from the Caenorhabditis Genetics Center (CGC). The worms were grown at 21°C. Stocks of *C. elegans* were acclimated to CeHR medium for three weeks prior to microgravity experiments. The ground control animals were maintained in CeHR medium in 20 mL scintillation vials as described [16]. Approximately 100,000 live worms (P_0 generation) were cleaned by sucrose floatation, their embryos (F_1 generation) were harvested by bleaching and placed in ~40 mL of CeHR culture in sterile VueLife culture bags ("AC" Series 32-C, Saint-Gobain). Culture bags were mounted in the clinostat and rotated at 1 rad/sec (~ 10 RPM) for four days, which is the measured time to reach L4/adulthood [19]. The "F_2" and subsequent generations were approximated by using four-day intervals. Prior to RNA extraction, only live worms are retrieved using the sucrose floatation method. We note that "F2" generation and beyond will not maintain synchronicity, and all will contain a mixture of generations, but recovering only the live animals enriches the RNA pool for the expected (majority) generation as each adult will produce ~30 offspring. The reason for the usage of mixed stage worms were the difficulties experienced (e.g., contamination of the liquid medium) during the synchronizing of the animals.

RNA isolation, Illumina sequencing

RNA isolation and RNA-seq was performed with triplicates on Illumina HiSeq 2500 in 50bp single-end reads as described previously [16]. As we achieved high correlation for gene expressions with both RNA-seq and qRT-PCR in our previous work [16], we did not perform a separate qRT-PCR for this study.

bioRxiv preprint doi: https://doi.org/10.1101/531335; this version posted January 26, 2019. The copyright holder for this preprint (which was not certified by peer review) is the author/funder, who has granted bioRxiv a license to display the preprint in perpetuity. It is made available under aCC-BY-NC-ND 4.0 International license.

Gene expression analysis

Quality control on the RNA-seq data was done with FASTQC (version 0.11.2) [64]. All the reads were in the "very good" quality range. The DEGs were identified by using two separate approaches. First, the Tuxedo pipeline [46] was used with default parameters. Second, the DESeq2 software (version 1.16.1)[47] was utilized after quantifying the expression of transcripts with Salmon (version 0.8.2)[65]. The reference genome (WBCel235) along with the annotation file were retrieved from Ensembl [66]. We considered genes as differentially expressed if FDR adjusted *p-values* < 0.05, and log2 fold change > 2 unless otherwise stated. The results from the Tuxedo pipeline was used throughout the paper as explained in the results and the results from DESeq2 were reported in the supplementary data (Additional File 1: Fig. S4; Additional File 7: Dataset S5). We discarded miRNA, piRNA, and rRNA molecules from the analysis. The ncRNA molecules (WS250) and unconfirmed genes were obtained from WormBase [31]. Dendrogram was generated with Ward's clustering criterion by using R software.

Functional analysis of the genes

Gene ontology (GO) enrichment for biological processes and protein domains were assessed with Database for Annotation, Visualization and Integrated Discovery (DAVID) (v6.8) [67]. The GO network for the common DEGs between our simulated microgravity experiment and CERISE4 was created in Cytoscape (version 3.4.0) [68] by using the BINGO plugin [69]. Pathway analysis was done using KEGG Mapper (https://www.genome.jp/kegg/tool/map_pathway1.html). Tissue enrichment analysis was performed by using WormBase Gene Set Enrichment Analysis tool [70], and FDR adj. p-value < 0.05 considered significant and top ten tissues were reported.

bioRxiv preprint doi: https://doi.org/10.1101/531335; this version posted January 26, 2019. The copyright holder for this preprint (which was not certified by peer review) is the author/funder, who has granted bioRxiv a license to display the preprint in perpetuity. It is made available under aCC-BY-NC-ND 4.0 International license.

Comparison of DEGs to the previous studies in *C. elegans*

NASA's GeneLab (https://genelab.nasa.gov/) platform was used to acquire the Gene Expression Omnibus (GEO) accession numbers for the previous studies on microgravity related gene expressions in *C. elegans*. We identified four such studies with the following GEO accession numbers: GSE71771 (Expression Data from International *C. elegans* Experiment 1st), GSE71770 (CERISE, 4 days), GSE27338 (CERISE, 8 days), and GSE32949 by UKM (PRJNA146465) from the query made on June 30, 2016 with "*C. elegans*" and "microgravity" terms on GeneLab. We analyzed these publicly available microarray datasets with GEO2R (https://www.ncbi.nlm.nih.gov/geo/geo2r/) for gene expressions under microgravity at the ISS versus 1G control in four and eight days CERISE and versus ground control conditions for the other two. The genes with logFC > 2 and Benjamini & Hochberg corrected p-value < 0.05 were considered as differentially expressed.

STRING database (version 10.5) [48] was used to determine whether the commonly DEGs from our simulated microgravity experiment and CERISE4 show enrichment for protein-protein interactions (PPI). We only considered the interactions only from experiments, gene-fusion, databases, and co-expression and selected "high-confidence (0.7)" results. PPI enrichment showed significance at *p-value* < 1.0e-16 with 58 interacting nodes and 155 edges. The PPI network was visualized with Cytoscape (version 3.4.0) [68]. Edge width was determined based on the "combined score" for the interactions obtained from the STRING database. We identified the human orthologs of the gravitome with OrthoList 2 with default settings [71].

Mass spectrometry for ceramides

The worms were chopped manually with razor blades on ice-cold glass. Three replicates for ground control and simulated microgravity conditions with mixed stage worms were used

bioRxiv preprint doi: https://doi.org/10.1101/531335; this version posted January 26, 2019. The copyright holder for this preprint (which was not certified by peer review) is the author/funder, who has granted bioRxiv a license to display the preprint in perpetuity. It is made available under aCC-BY-NC-ND 4.0 International license.

514 simultaneously. Each sample was sent to Avanti Polar Lipids Analytical Services as a frozen
515 extract in glass tubes for liquid chromatography with tandem mass spectrometry (LC/MS/MS)
516 experiment for detection of Ceramide levels. Each sample was extracted by modified Bligh and
517 Dyer extraction. The samples were dried and resolvated in 50:50 Chloroform:Methanol and
518 diluted prior to analysis. The resolvated sample was used for analyses and stored at -20°C until
519 assayed. Samples were diluted as needed for analysis with internal standards for Ceramides for
520 quantization by injection on LC/MS/MS. The individual molecular species for each sphingolipid
521 group were measured by reversed phased liquid chromatography tandem mass spectrometry
522 methods which separate the compounds by multiple reaction monitoring m/z to fragments and
523 retention time. Quantification was performed by ratio of analyte to internal standard response
524 multiplied by ISTD concentration and m/z response correction factor. The results are expressed
525 as ng/rnl. The consistency among the replicates were examined with Pearson correlation. All but
526 one replicates in both the experiments showed high correlation ($R^2 > 0.9$). The ground control
527 replicate which did not show a strong correlation (around 60%) with the other replicates was
528 excluded from the analysis. The data were analyzed with t-test (two-tailed), and *p-value* < 0.05
529 was considered significant. Equal variances were confirmed with Levene's test at $\alpha = 0.05$ for all
530 the ceramides tested.

531

532 ## Microgravity simulation with clinorotation

533 We used a lab-built clinostat with integrated microscope to observe the motion of small objects
534 including microspheres, yeast cells and *C. elegans* embryos during clinorotation. The trajectory
535 of a spherical particle in a rotating vessel have been described previously in literature [2, 8, 72,
536 73]. Dedolph and Dipert (1971) separated the motion of a spherical particle into two parts: a

bioRxiv preprint doi: https://doi.org/10.1101/531335; this version posted January 26, 2019. The copyright holder for this preprint (which was not certified by peer review) is the author/funder, who has granted bioRxiv a license to display the preprint in perpetuity. It is made available under aCC-BY-NC-ND 4.0 International license.

circular motion under the influence of gravity, the radius of which is inversely proportion to the angular velocity (ω, rad/sec), and a radial motion due to centrifugal forces, the velocity of which is proportional to ω^2 [72]. The equation of motion that describes the orbital trajectories is given by:

$$m\frac{d^2q}{dx^2} + (2i\omega m + \lambda)\frac{dq}{dt} - \omega^2(m - m_w)q = -ig(m - m_w)e^{-i\omega t}.$$

In the above equation, λ is the viscous drag coefficient, m is the mass of the object, m_w is the mass of the displaced water, t is time, g is the acceleration due to gravity, and $q(x,y,z,t)$ is the rotating reference frame defined as:

$$q \equiv x_{rot} + iy_{rot} = ze^{-i\omega t}.$$

As a test of the performance of the clinostat we recorded the motion of fluorescent melamine-formaldehyde microspheres (5.6 µm diameter, 1.51 g/cm^3 density; Corpuscular Inc., Cold Harbor, NY) suspended in a 3% bovine serum albumin (BSA) solution (Additional file 10: Movie S2). This solution was injected into an 8-mm diameter, 100-µm deep, coverglass topped chamber mounted on the clinostat microscope. Some of the melamine microspheres adhere to coverglass of the chamber, conveniently providing fiducial markers which we were able to use to compensate for the mechanical noise introduced into the micrographs by the rotation of the clinostat. We measured the terminal velocity of the suspended microspheres to be 3.2 ± 0.2 µm/s (mean ± SEM, n = 8). Figure S6 shows a plot of the measured radius of circular motion of suspended microspheres as a function of inverse angular velocity (black dots), and the calculated radius [2] using the measured mean terminal velocity (blue line). The shaded area encompasses calculated radii for terminal velocities within one standard deviation of the mean.

bioRxiv preprint doi: https://doi.org/10.1101/531335; this version posted January 26, 2019. The copyright holder for this preprint (which was not certified by peer review) is the author/funder, who has granted bioRxiv a license to display the preprint in perpetuity. It is made available under aCC-BY-NC-ND 4.0 International license.

Abbreviations

CeHR: *C. elegans* Habitation and Reproduction

CeMM: *C. elegans* Maintenance Medium

DAVID: Database for Annotation, Visualization and Integrated Discovery

DEG: Differentially expressed gene

FDR: False discovery rate

FPKM: Fragments Per Kilobase of transcript per Million mapped reads

GO: Gene ontology

ncRNA: Non-coding RNA

RNA-seq: RNA-sequencing

GC: Ground control

MG: Simulated microgravity

R1_GC: Four days after return to ground conditions

R2_GC: Eight days after return to ground conditions

R3_GC: Twelve days after return to ground conditions

Acknowledgements

We are grateful to Michael Moore for his help developing the clinostat. İÇ thanks the colleagues from Comparative and Experimental Approaches to Aging Biology course in the MDI Biological

bioRxiv preprint doi: https://doi.org/10.1101/531335; this version posted January 26, 2019. The copyright holder for this preprint (which was not certified by peer review) is the author/funder, who has granted bioRxiv a license to display the preprint in perpetuity. It is made available under aCC-BY-NC-ND 4.0 International license.

574 Laboratory for helpful discussions. İÇ acknowledges the University of Delaware for Dissertation
575 Fellowship and Graduate Fellow Award.

576 Funding

577 This work was supported by NASA grants NNX12AR59G, NNX10AN63H, and
578 NNX13AM08G, awarded to CRS and Sigma Xi grant G2016100191301836, awarded to İÇ. The
579 BIOMIX computing cluster and the Bioimaging center are supported by Delaware INBRE grant
580 (NIH/NIGMS GM103446) and Delaware EPSCoR grants (NSF EPS-0814251 and NSF IIA-
581 1330446). None of these funding bodies were involved in the design, data collection, analysis,
582 interpretation of data, or in writing the manuscript.

583 Authors' contributions

584 İÇ and CRS designed the study. AJ developed the clinostat. İÇ and JHD conducted the
585 experiments. İÇ performed the analyses and interpreted the results. İÇ, AJ, and CRS wrote the
586 manuscript. All authors read and approved the final manuscript.

587 Ethics approval and consent to participate

588 Not applicable as *C. elegans* do not require ethical permits or consent to participate.

589 Consent for publication

590 Not applicable.

591 Competing interests

592 The authors declare that they have no competing interests.

bioRxiv preprint doi: https://doi.org/10.1101/531335; this version posted January 26, 2019. The copyright holder for this preprint (which was not certified by peer review) is the author/funder, who has granted bioRxiv a license to display the preprint in perpetuity. It is made available under aCC-BY-NC-ND 4.0 International license.

Figure Legends:

Fig. 1: Transcriptomic response of *C. elegans* to simulated microgravity and return to ground conditions. **(A)** Clinostat used for simulating microgravity. **(B)** Experimental design for the effect of simulated microgravity on gene expressions during the exposure and after the return. **(C)** Dendrogram of the gene expression profiles for ground condition (GC), simulated microgravity (MG), four days after return to ground conditions (R1_GC), eight days after return to ground conditions (R2_GC), and twelve days after return to ground conditions (R3_GC). **(D)** Log2 fold change of the gene expressions (FPKM) between the conditions.

Fig. 2: Differentially expressed gene profiles under simulated microgravity and after return to ground conditions. **(A)** Tissue enrichment of the upregulated (green) and downregulated (red) genes under simulated microgravity. **(B)** Pathway enrichment of the upregulated (green) and downregulated (red) genes during the exposure to simulated microgravity (MG), and four and eight days after return to ground conditions (R1 GC and R2 GC, respectively). **(C)** The number differentially expressed genes under simulated microgravity and the transmission of the differential expression after return to ground conditions. **(D)** Categorization of the upregulated genes in comparison to the ground control animals, and the enriched gene ontology terms assigned to them. **(E)** Categorization of the downregulated genes in comparison to the ground control animals, and the enriched gene ontology terms assigned to them.

Fig. 3: Longevity regulating pathway genes are differentially expressed under simulated microgravity. Adopted from the KEGG longevity regulating pathway – worm (cel04212).

Fig. 4: Sphingolipid signaling pathway is downregulated under simulated microgravity. **(A)** The sphingolipid signaling pathway genes *asah-1*, *asm-3*, and *gba-4* are downregulated under simulated microgravity. The downregulation pattern of *asm-3* and *gba-4* is maintained for eight days after return to ground conditions. **(B)** The levels of d18:1 sphingosine, total ceramide, hexosylceramide, and sphingoid base reduced while total lactosylceramide level increased under simulated microgravity. **(C)** The levels of different acyl-chain ceramides show alterations under simulated microgravity. The error bars represent the standard error of the mean (* $p < 0.05$, ** $p < 0.01$, *** $p < 0.001$)

Fig. 5: Gravitome genes are consistently differentially expressed in the ISS and under simulated microgravity. **(A)** Shared DEGs among the space-flown worms and our simulated microgravity experiment. The highest number of common DEGs are between our experiment and four-day CERISE. These genes are named as the "gravitome". **(B)** The hierarchical clustering of the overall gene expressions among the space-flown worms and our simulated microgravity experiment. Our results analyzed with two different data analysis pipelines demonstrated highly similar patterns. **(C)** The number common of DEGs were high for our results analyzed with two different pipelines. Both of the pipelines showed common number of DEGs are higher that the values expected by chance (hypergeometric text, $p < 0.05$). **(D)** Protein-protein interaction of the gravitome genes from STRING database. **(E)** Gene ontology enrichment of the gravitome genes. **(F)** Protein domain enrichment of the gravitome genes.

bioRxiv preprint doi: https://doi.org/10.1101/531335; this version posted January 26, 2019. The copyright holder for this preprint (which was not certified by peer review) is the author/funder, who has granted bioRxiv a license to display the preprint in perpetuity. It is made available under aCC-BY-NC-ND 4.0 International license.

References

1. Sachs J. Lectures on the physiology of plants,. Oxford: Clarendon Press,; 1887.

2. Kessler J. The internal dynamics of slowly rotating biological systems. ASGSB Bull. 1992;5:11–21.

3. Dedolph RR, Oemick D a, Wilson BR, Smith GR. Causal basis of gravity stimulus nullification by clinostat rotation. Plant Physiol. 1967;42:1373–83.

4. Gruener R, Hoeger G. Vector-averaged gravity alters myocyte and neuron properties in cell culture. Aviat Space Environ Med. 1991;62:1159–65.

5. Wuest SL, Stern P, Casartelli E, Egli M. Fluid dynamics appearing during simulated microgravity using Random Positioning Machines. PLoS One. 2017;12.

6. Sievers A, Hejnowicz Z. How well does the clinostat mimic the effect of microgravity on plant cells and organs? ASGSB Bull. 1992;5:69–75.

7. Brown AH, Dahl AO, Chapman DK. Limitation on the Use of the Horizontal Clinostat as a Gravity Compensator. PLANT Physiol. 1976;58:127–30.

8. Briegleb W. Some qualitative and quantitative aspects of the fast-rotating clinostat as a research tool. ASGSB Bull. 1992;5:23–30.

9. Hemmersbach R, Volkmann D, Häder D-P. Graviorientation in Protists and Plants. J Plant Physiol. 1999;154:1–15.

10. Häder D-P, Hemmersbach R, Lebert M. Gravity and the Behavior of Unicellular Organisms. Cambridge: Cambridge University Press; 2005.

11. Çelen İ, Doh JH, Sabanayagam C. Genetic Adaptation of C. elegans to Environment Changes I: Multigenerational Analysis of the Transcriptome. doi.org. 2017;:194506. doi:10.1101/194506.

bioRxiv preprint doi: https://doi.org/10.1101/531335; this version posted January 26, 2019. The copyright holder for this preprint (which was not certified by peer review) is the author/funder, who has granted bioRxiv a license to display the preprint in perpetuity. It is made available under aCC-BY-NC-ND 4.0 International license.

654 12. Félix M-A, Braendle C. The natural history of Caenorhabditis elegans. Curr Biol. 2010;20:R965-9.

655 13. Lehner B, Crombie C, Tischler J, Fortunato A, Fraser AG. Systematic mapping of genetic interactions
656 in Caenorhabditis elegans identifies common modifiers of diverse signaling pathways. Nat Genet.
657 2006;38:896–903.

658 14. Hunt-Newbury R, Viveiros R, Johnsen R, Mah A, Anastas D, Fang L, et al. High-throughput in vivo
659 analysis of gene expression in Caenorhabditis elegans. PLoS Biol. 2007;5:e237.
660 doi:10.1371/journal.pbio.0050237.

661 15. Watson E, Walhout AJM. Caenorhabditis elegans metabolic gene regulatory networks govern the
662 cellular economy. Trends in Endocrinology and Metabolism. 2014;25:502–8.

663 16. Çelen İ, Doh JH, Sabanayagam CR. Effects of liquid cultivation on gene expression and phenotype of
664 C. elegans. BMC Genomics. 2018;19:562. doi:10.1186/s12864-018-4948-7.

665 17. Szewczyk NJ, Udranszky IA, Kozak E, Sunga J, Kim SK, Jacobson LA, et al. Delayed development
666 and lifespan extension as features of metabolic lifestyle alteration in C. elegans under dietary restriction. J
667 Exp Biol. 2006;209 Pt 20:4129–39. doi:10.1242/jeb.02492.

668 18. Zhao S, Fung-Leung WP, Bittner A, Ngo K, Liu X. Comparison of RNA-Seq and microarray in
669 transcriptome profiling of activated T cells. PLoS One. 2014;9.

670 19. Doh JH, Moore AB, Çelen İ, Moore MT, Sabanayagam CR. ChIP and Chips□: Introducing the
671 WormPharm for correlative studies employing pharmacology and genome-wide analyses in C . elegans. J
672 Biol Methods. 2016;3:1–11.

673 20. Higashibata A, Szewczyk NJ, Conley CA, Imamizo-Sato M, Higashitani A, Ishioka N. Decreased
674 expression of myogenic transcription factors and myosin heavy chains in Caenorhabditis elegans muscles
675 developed during spaceflight. J Exp Biol. 2006;209 Pt 16:3209–18. doi:10.1242/jeb.02365.

676 21. Qiao L, Luo S, Liu Y, Li X, Wang G, Huang Z. Reproductive and locomotory capacities of

bioRxiv preprint doi: https://doi.org/10.1101/531335; this version posted January 26, 2019. The copyright holder for this preprint (which was not certified by peer review) is the author/funder, who has granted bioRxiv a license to display the preprint in perpetuity. It is made available under aCC-BY-NC-ND 4.0 International license.

677 Caenorhabditis elegans were not affected by simulated variable gravities and spaceflight during the
678 Shenzhou-8 mission. Astrobiology. 2013;13:617–25. doi:10.1089/ast.2012.0962.

679 22. Tee LF, Neoh H min, Then SM, Murad NA, Asillam MF, Hashim MH, et al. Effects of simulated
680 microgravity on gene expression and biological phenotypes of a single generation Caenorhabditis elegans
681 cultured on 2 different media. Life Sci Sp Res. 2017;15:11–7.

682 23. Reinke V, Krause M, Okkema P. Transcriptional regulation of gene expression in C. elegans.
683 WormBook. 2013;:1–34. doi:10.1895/wormbook.1.45.2.

684 24. Honda Y, Honda S, Narici M, Szewczyk NJ. Spaceflight and ageing: reflecting on Caenorhabditis
685 elegans in space. Gerontology. 2014;60:138–42. doi:10.1159/000354772.

686 25. Honda Y, Higashibata A, Matsunaga Y, Yonezawa Y, Kawano T, Higashitani A, et al. Genes down-
687 regulated in spaceflight are involved in the control of longevity in Caenorhabditis elegans. Sci Rep.
688 2012;2:413–29. doi:10.1038/srep00487.

689 26. Lin K, Hsin H, Libina N, Kenyon C. Regulation of the Caenorhabditis elegans longevity protein
690 DAF-16 by insulin/IGF-1 and germline signaling. Nat Genet. 2001;28:139–45.

691 27. Seung WO, Mukhopadhyay A, Dixit BL, Raha T, Green MR, Tissenbaum HA. Identification of direct
692 DAF-16 targets controlling longevity, metabolism and diapause by chromatin immunoprecipitation. Nat
693 Genet. 2006;38:251–7.

694 28. Murphy CT, McCarroll SA, Bargmann CI, Fraser A, Kamath RS, Ahringer J, et al. Genes that act
695 downstream of DAF-16 to influence the lifespan of Caenorhabditis elegans. Nature. 2003;424:277–84.

696 29. Lee SS, Kennedy S, Tolonen AC, Ruvkun G. DAF-16 target genes that control C. elegans Life-span
697 and metabolism. Science (80-). 2003;300:644–7.

698 30. Tepper RG, Ashraf J, Kaletsky R, Kleemann G, Murphy CT, Bussemaker HJ. PQM-1 complements
699 DAF-16 as a key transcriptional regulator of DAF-2-mediated development and longevity. Cell.

bioRxiv preprint doi: https://doi.org/10.1101/531335; this version posted January 26, 2019. The copyright holder for this preprint (which was not certified by peer review) is the author/funder, who has granted bioRxiv a license to display the preprint in perpetuity. It is made available under aCC-BY-NC-ND 4.0 International license.

2013;154:676–90.

31. Harris TW, Baran J, Bieri T, Cabunoc A, Chan J, Chen WJ, et al. WormBase 2014: new views of curated biology. Nucleic Acids Res. 2014;42 Database issue:D789-93. doi:10.1093/nar/gkt1063.

32. Cui M, Wang Y, Cavaleri J, Kelson T, Teng Y, Han M. Starvation-induced stress response is critically impacted by ceramide levels in Caenorhabditis elegans. Genetics. 2017;205:775–85.

33. Kim Y, Sun H. ASM-3 Acid Sphingomyelinase Functions as a Positive Regulator of the DAF-2/AGE-1 Signaling Pathway and Serves as a Novel Anti-Aging Target. PLoS One. 2012;7:e45890. doi:10.1371/journal.pone.0045890.

34. Cutler RG, Thompson KW, Camandola S, Mack KT, Mattson MP. Sphingolipid metabolism regulates development and lifespan in Caenorhabditis elegans. Mech Ageing Dev. 2014;143–144:9–18. doi:10.1016/j.mad.2014.11.002.

35. Huang X, Withers BR, Dickson RC. Sphingolipids and lifespan regulation. Biochimica et Biophysica Acta - Molecular and Cell Biology of Lipids. 2014;1841:657–64.

36. Hernández-Corbacho MJ, Jenkins RW, Clarke CJ, Hannun YA, Obeid LM, Snider AJ, et al. Accumulation of long-chain glycosphingolipids during aging is prevented by caloric restriction. PLoS One. 2011;6.

37. Straczkowski M, Kowalska I. The role of skeletal muscle sphingolipids in the development of insulin resistance. Review of Diabetic Studies. 2008;5:13–24.

38. Bismuth J, Lin P, Yao Q, Chen C. Ceramide: A common pathway for atherosclerosis? Atherosclerosis. 2008;196:497–504.

39. Chan JP, Brown J, Hark B, Nolan A, Servello D, Hrobuchak H, et al. Loss of sphingosine kinase alters life history traits and locomotor function in Caenorhabditis elegans. Front Genet. 2017;8 SEP.

bioRxiv preprint doi: https://doi.org/10.1101/531335; this version posted January 26, 2019. The copyright holder for this preprint (which was not certified by peer review) is the author/funder, who has granted bioRxiv a license to display the preprint in perpetuity. It is made available under aCC-BY-NC-ND 4.0 International license.

722 40. Menuz V, Howell KS, Gentina S, Epstein S, Riezman I, Fornallaz-Mulhauser M, et al. Protection of
723 C. elegans from Anoxia by HYL-2 ceramide synthase. Science (80-). 2009;324:381–4.

724 41. Deng X, Yin X, Allan R, Lu DD, Maurer CW, Haimovitz-Friedman A, et al. Ceramide biogenesis is
725 required for radiation-induced apoptosis in the germ line of C. elegans. Science (80-). 2008;322:110–5.

726 42. Higashitani A, Hashizume T, Sugimoto T, Mori C, Nemoto K, Etheridge T, et al. C. elegans RNAi
727 space experiment (CERISE) in Japanese Experiment Module KIBO. Biol Sci Sp. 2009;23:183–7.
728 doi:10.2187/bss.23.183.

729 43. Samuel TK, Sinclair JW, Pinter KL, Hamza I. Culturing Caenorhabditis elegans in axenic liquid
730 media and creation of transgenic worms by microparticle bombardment. J Vis Exp. 2014;:e51796.
731 doi:10.3791/51796.

732 44. Higashibata A, Hashizume T, Nemoto K, Higashitani N, Etheridge T, Mori C, et al. Microgravity
733 elicits reproducible alterations in cytoskeletal and metabolic gene and protein expression in space-flown
734 Caenorhabditis elegans. npj Microgravity. 2016;2:15022. doi:10.1038/npjmgrav.2015.22.

735 45. Then, S. M., Jusoh, N. F., Harun, R., Nathan, S., Szewczyk, N. J., Stodieck, L., & Jamal R. Multi-
736 Generational Culture of C. Elegans on a Long-Term Space Flight Revealed Changes in Expression of
737 Genes Involved in Longevity, DNA Repair, and Locomotion. Asia-Pacific J Mol Med. 2016;4:1.
738 http://spaj.ukm.my/apjmm/index.php/apjmm/article/view/20.

739 46. Trapnell C, Roberts A, Goff L, Pertea G, Kim D, Kelley DR, et al. Differential gene and transcript
740 expression analysis of RNA-seq experiments with TopHat and Cufflinks. Nat Protoc. 2012;7:562–78.
741 doi:10.1038/nprot.2012.016.

742 47. Love MI, Huber W, Anders S. Moderated estimation of fold change and dispersion for RNA-seq data
743 with DESeq2. Genome Biol. 2014;15.

744 48. Szklarczyk D, Morris JH, Cook H, Kuhn M, Wyder S, Simonovic M, et al. The STRING database in

bioRxiv preprint doi: https://doi.org/10.1101/531335; this version posted January 26, 2019. The copyright holder for this preprint (which was not certified by peer review) is the author/funder, who has granted bioRxiv a license to display the preprint in perpetuity. It is made available under aCC-BY-NC-ND 4.0 International license.

745 2017: Quality-controlled protein-protein association networks, made broadly accessible. Nucleic Acids
746 Res. 2017;45:D362–8.

747 49. Gao Y, Arfat Y, Wang H, Goswami N. Muscle atrophy induced by mechanical unloading:
748 Mechanisms and potential countermeasures. Frontiers in Physiology. 2018.

749 50. Salazar JJ, Michele DE, Brooks S V. Inhibition of calpain prevents muscle weakness and disruption
750 of sarcomere structure during hindlimb suspension. J Appl Physiol. 2010.

751 51. Seale P, Bjork B, Yang W, Kajimura S, Chin S, Kuang S, et al. PRDM16 controls a brown fat/skeletal
752 muscle switch. Nature. 2008;454:961–7.

753 52. Cutler RG, Pedersen WA, Camandola S, Rothstein JD, Mattson MP. Evidence that accumulation of
754 ceramides and cholesterol esters mediates oxidative stress - Induced death of motor neurons in
755 amyotrophic lateral sclerosis. Ann Neurol. 2002;52:448–57.

756 53. Graveley A, Vlasov A, Freeman A, Wu K, Szewczyk NJ, D'Cruz R, et al. Levels of acid
757 sphingomyelinase (ASM) in Caenorhabditis elegans in microgravity. Gravitational Sp Res. 2018;6(1):27–
758 36. http://gravitationalandspacebiology.org/index.php/journal/article/viewFile/803/809. Accessed 9 Oct
759 2018.

760 54. Edwards M, Abadie L. NASA Twins Study Investigators to Release Integrated Paper in 2018. 2018.
761 https://www.nasa.gov/feature/nasa-twins-study-investigators-to-release-integrated-paper-in-2018.
762 Accessed 9 Oct 2018.

763 55. Sahin E, Depinho RA. Linking functional decline of telomeres, mitochondria and stem cells during
764 ageing. Nature. 2010;464:520–8.

765 56. Joeng KS, Song EJ, Lee KJ, Lee J. Long lifespan in worms with long telomeric DNA. Nat Genet.
766 2004;36:607–11.

767 57. Monaghan P. Telomeres and life histories: The long and the short of it. Annals of the New York

bioRxiv preprint doi: https://doi.org/10.1101/531335; this version posted January 26, 2019. The copyright holder for this preprint (which was not certified by peer review) is the author/funder, who has granted bioRxiv a license to display the preprint in perpetuity. It is made available under aCC-BY-NC-ND 4.0 International license.

768 Academy of Sciences. 2010;1206:130–42.

769 58. Heidinger BJ, Blount JD, Boner W, Griffiths K, Metcalfe NB, Monaghan P. Telomere length in early
770 life predicts lifespan. Proc Natl Acad Sci. 2012;109:1743–8. doi:10.1073/pnas.1113306109.

771 59. Saddoughi SA, Song P, Ogretmen B. Roles of Bioactive Sphingolipids in Cancer Biology and
772 Therapeutics. In: Lipids in Health and Disease. Dordrecht: Springer Netherlands; 2008. p. 413–40.
773 doi:10.1007/978-1-4020-8831-5_16.

774 60. Honda Y, Honda S, Narici M, Szewczyk NJ. Spaceflight and Ageing: Reflecting on *Caenorhabditis*
775 *elegans* in Space. Gerontology. 2014;60:138–42. doi:10.1159/000354772.

776 61. Taylor PW. Impact of space flight on bacterial virulence and antibiotic susceptibility. Infection and
777 Drug Resistance. 2015.

778 62. Spencer WC, Zeller G, Watson JD, Henz SR, Watkins KL, McWhirter RD, et al. A spatial and
779 temporal map of C. elegans gene expression. Genome Res. 2011;21:325–41.

780 63. Adenle AA, Johnsen B, Szewczyk NJ. Review of the results from the International C. elegans first
781 experiment (ICE-FIRST). Advances in Space Research. 2009;44:210–6.

782 64. Andrews S. FastQC: A quality control tool for high throughput sequence data. Available at:
783 www.bioinformatics.babraham.ac.uk/projects/fastqc/. FastQC: A quality control tool for high throughput
784 sequence data. Available at: www.bioinformatics.babraham.ac.uk/projects/fastqc/. 2010.

785 65. Patro R, Duggal G, Love MI, Irizarry RA, Kingsford C. Salmon provides fast and bias-aware
786 quantification of transcript expression. Nature Methods. 2017.

787 66. Cunningham F, Amode MR, Barrell D, Beal K, Billis K, Brent S, et al. Ensembl 2015. Nucleic Acids
788 Res. 2014;43:D662-669. doi:10.1093/nar/gku1010.

789 67. Huang DW, Sherman BT, Lempicki RA. Systematic and integrative analysis of large gene lists using

bioRxiv preprint doi: https://doi.org/10.1101/531335; this version posted January 26, 2019. The copyright holder for this preprint (which was not certified by peer review) is the author/funder, who has granted bioRxiv a license to display the preprint in perpetuity. It is made available under aCC-BY-NC-ND 4.0 International license.

790 DAVID bioinformatics resources. Nat Protoc. 2008;4:44–57. doi:10.1038/nprot.2008.211.

791 68. Shannon P, Markiel A, Ozier O, Baliga NS, Wang JT, Ramage D, et al. Cytoscape: a software
792 environment for integrated models of biomolecular interaction networks. Genome Res. 2003;13:2498–
793 504. doi:10.1101/gr.1239303.

794 69. Maere S, Heymans K, Kuiper M. BiNGO: a Cytoscape plugin to assess overrepresentation of gene
795 ontology categories in biological networks. Bioinformatics. 2005;21:3448–9.
796 doi:10.1093/bioinformatics/bti551.

797 70. Angeles-Albores D, N. Lee RY, Chan J, Sternberg PW. Tissue enrichment analysis for C. elegans
798 genomics. BMC Bioinformatics. 2016;17:366. doi:10.1186/s12859-016-1229-9.

799 71. Kim W, Underwood RS, Greenwald I, Shaye DD. OrthoList 2: A New Comparative Genomic
800 Analysis of Human and Caenorhabditiselegans Genes. Genetics. 2018;:genetics.301307.2018.
801 doi:10.1534/genetics.118.301307.

802 72. Dedolph RR, Dipert MH. The physical basis of gravity stimulus nullification by clinostat rotation.
803 Plant Physiol. 1971;47:756–64.

804 73. Lee Silver I. The dynamics of a discrete geotropic sensor subject to rotation-induced gravity
805 compensation. J Theor Biol. 1976;61:353–62.

806

807

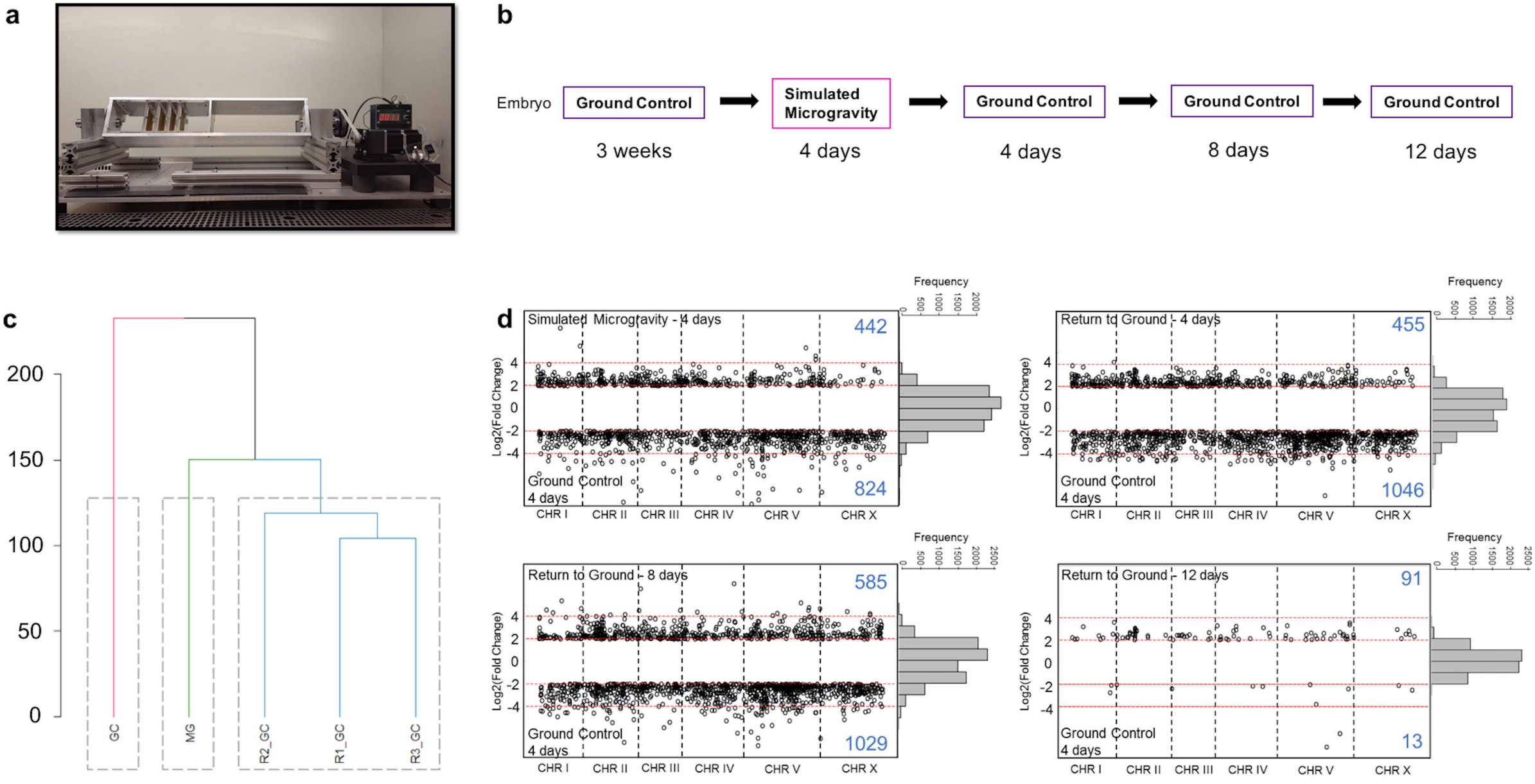
a
b
Embryo
Ground Control
3 weeks
Simulated Microgravity
4 days
Ground Control
4 days
Ground Control
8 days
Ground Control
12 days
c
Height
200
150
100
50
0
GC
MG
R2_GC
R1_GC
R3_GC
d
Simulated Microgravity - 4 days
442
Ground Control 4 days
824
Return to Ground - 4 days
455
Ground Control 4 days
1046
Return to Ground - 8 days
585
Ground Control 4 days
1029
Return to Ground - 12 days
91
Ground Control 4 days
13
Log2(Fold Change)
Frequency
CHR I
CHR II
CHR III
CHR IV
CHR V
CHR X

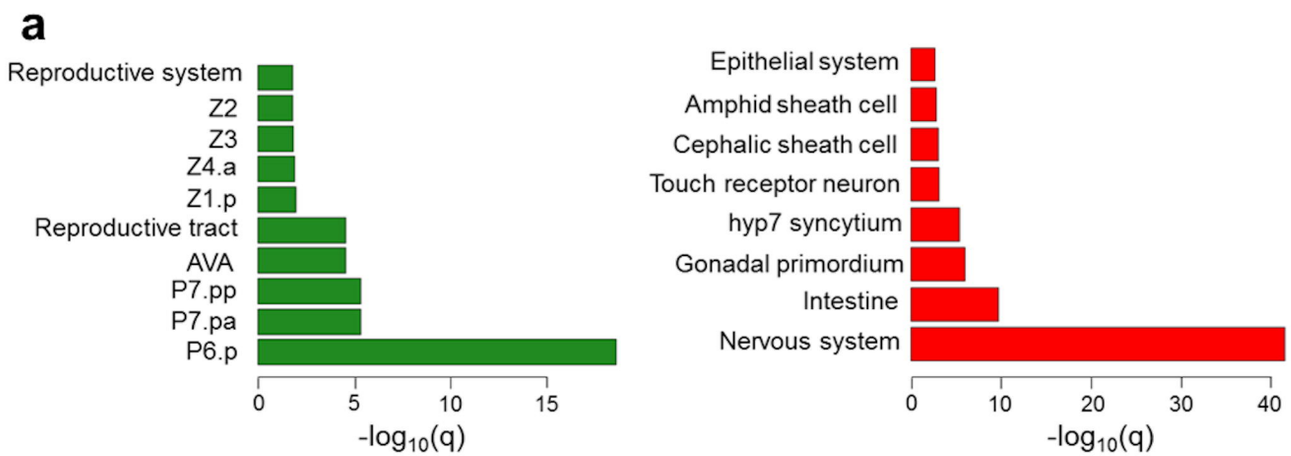

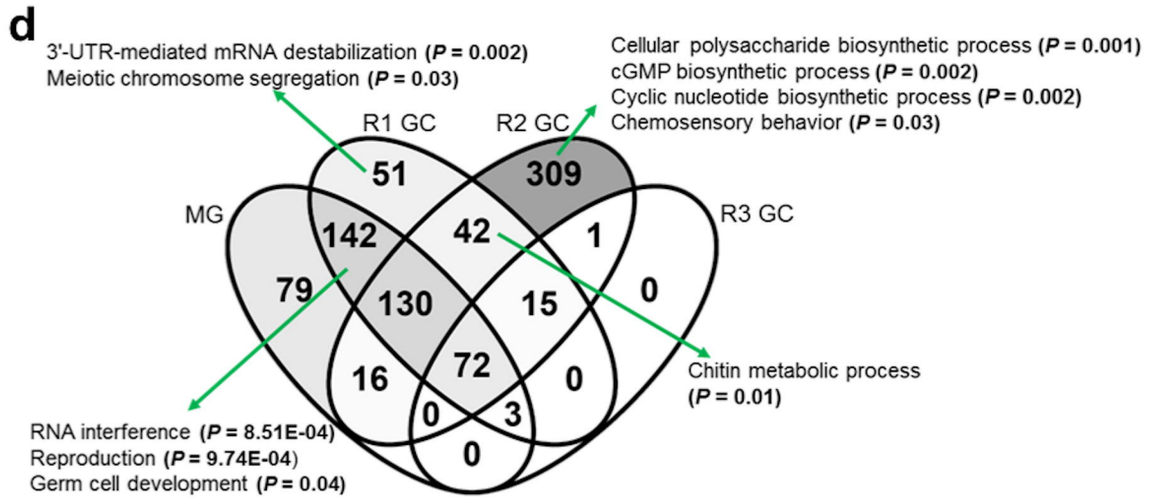

b

	Pathway		P-value
MG	Dorso-ventral axis formation	↑	4.3e-5
	Lysosome	↓	5.4e-6
R1 GC	Dorso-ventral axis formation	↑	3.6e-2
	Lysosome	↓	1.9e-5
R2 GC	Metabolic process	↓	9.0e-4
	Lysosome	↓	5.5e-4
	Drug metabolism –cytochrome P450	↓	1.9e-2

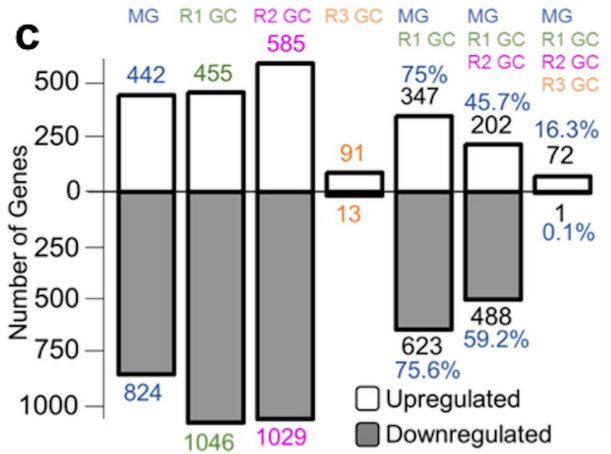

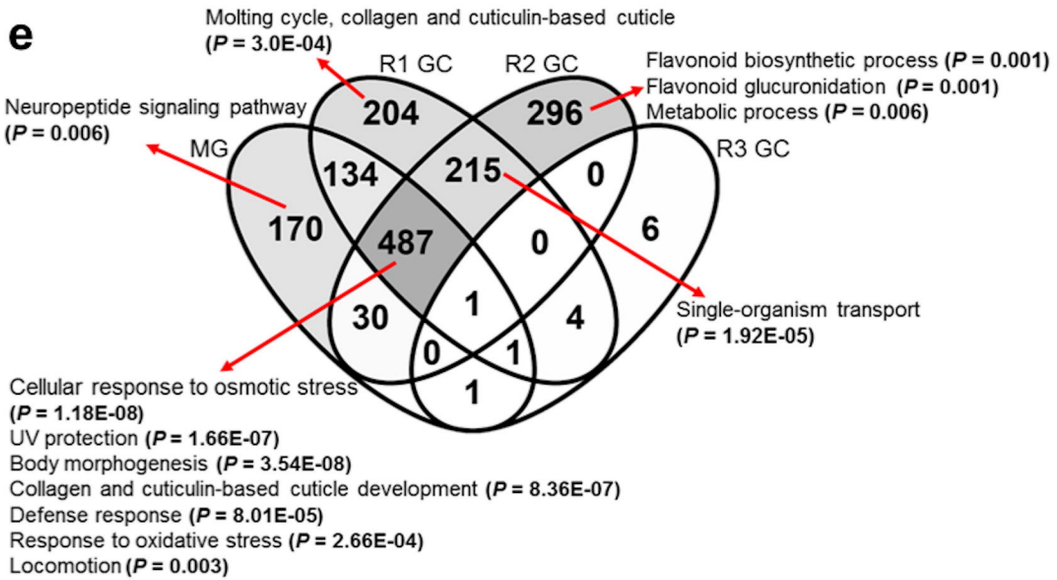

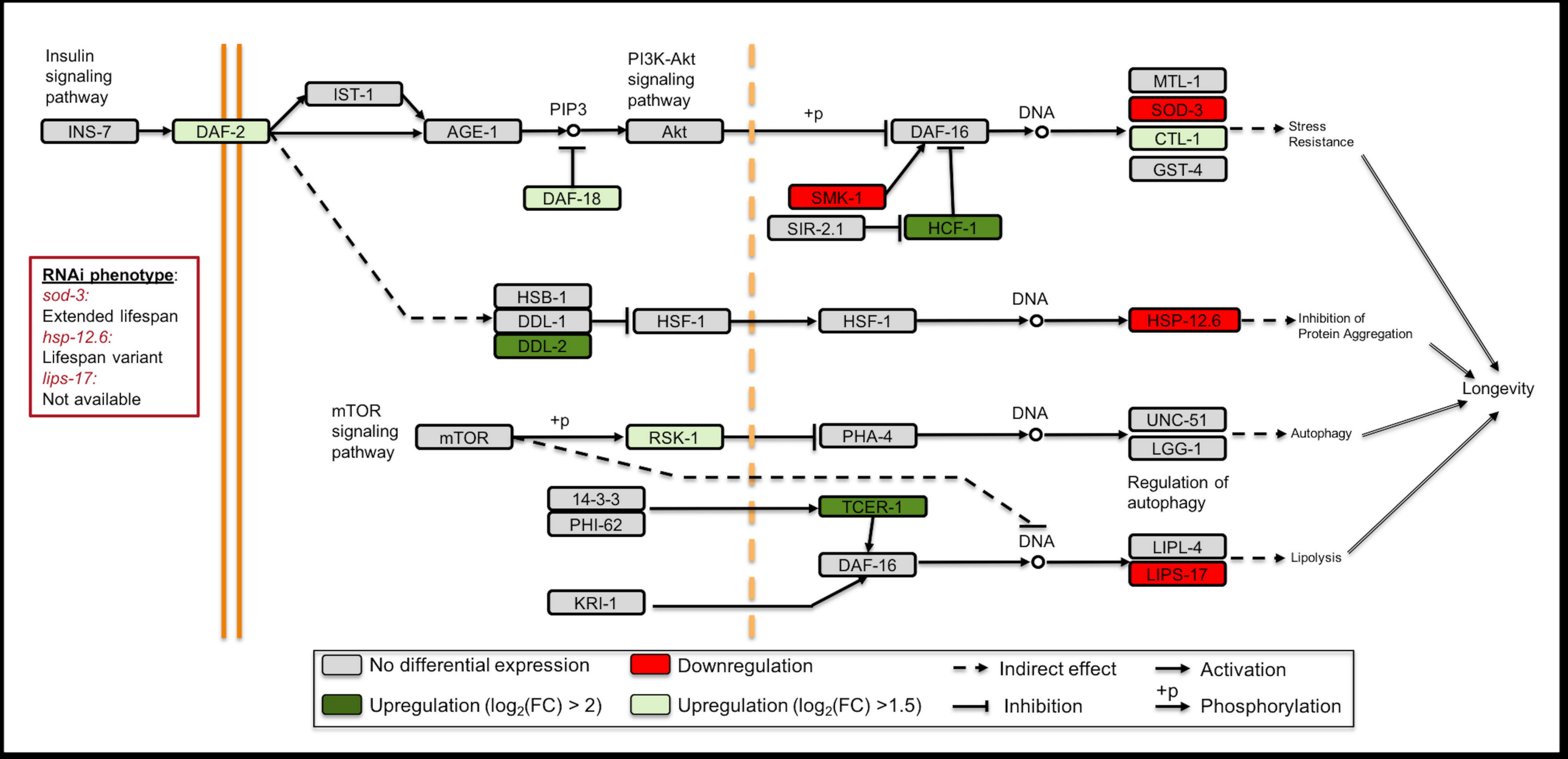
Insulin signaling pathway
INS-7
DAF-2
IST-1
AGE-1
PIP3
DAF-18
PI3K-Akt signaling pathway
Akt
+p
DAF-16
DNA
MTL-1
SOD-3
CTL-1
GST-4
Stress Resistance
SMK-1
SIR-2.1
HCF-1
RNAi phenotype:
sod-3:
Extended lifespan
hsp-12.6:
Lifespan variant
lips-17:
Not available
HSB-1
DDL-1
DDL-2
HSF-1
HSF-1
DNA
HSP-12.6
Inhibition of Protein Aggregation
Longevity
mTOR signaling pathway
mTOR
+p
RSK-1
PHA-4
DNA
UNC-51
LGG-1
Autophagy
Regulation of autophagy
14-3-3
PHI-62
TCER-1
DAF-16
DNA
LIPL-4
LIPS-17
Lipolysis
KRI-1
No differential expression
Downregulation
Indirect effect
Activation
Upregulation (log2(FC) > 2)
Upregulation (log2(FC) >1.5)
Inhibition
+p
Phosphorylation

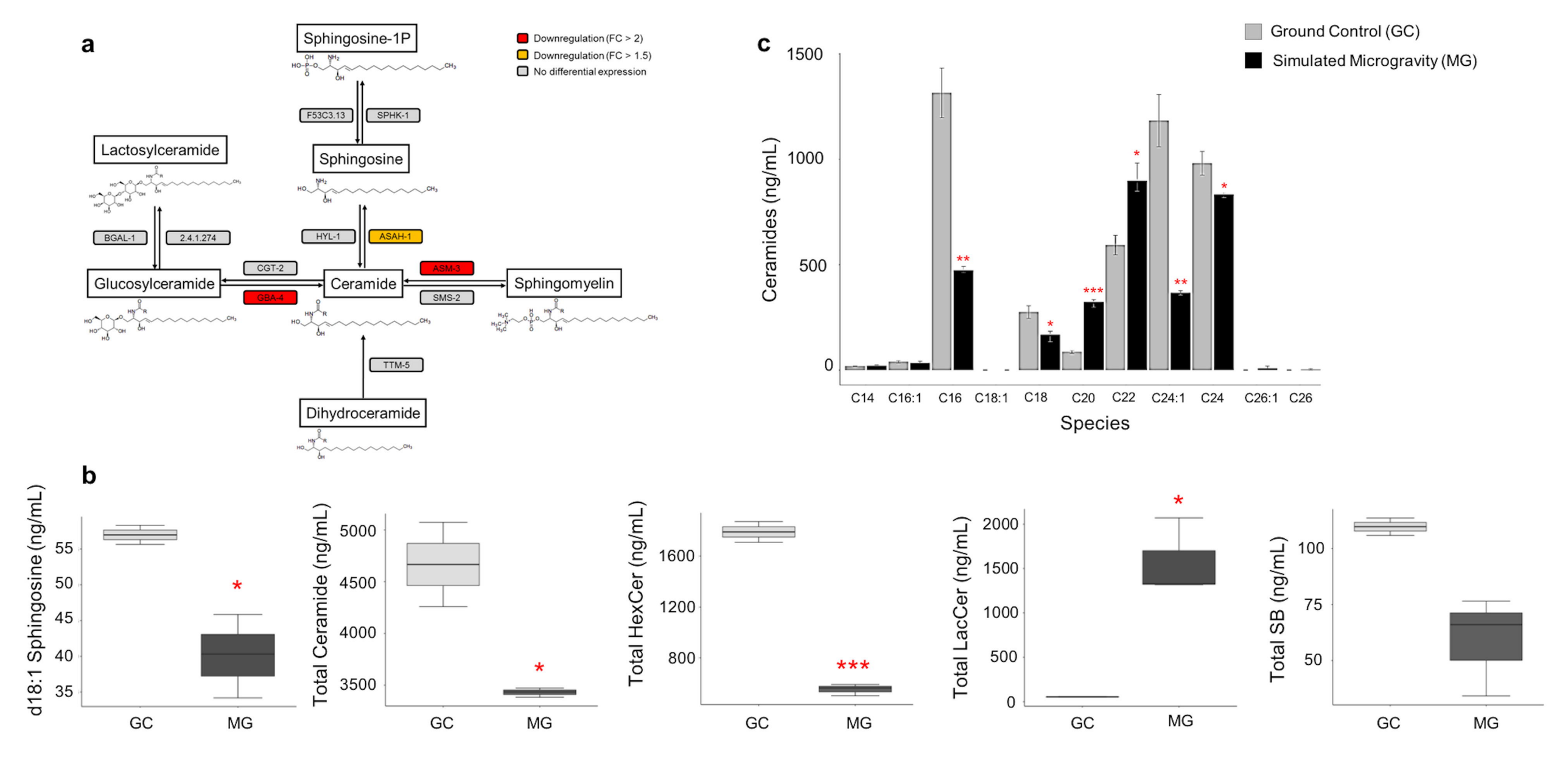
a
Sphingosine-1P
Downregulation (FC > 2)
Downregulation (FC > 1.5)
No differential expression
F53C3.13
SPHK-1
Lactosylceramide
Sphingosine
BGAL-1
2.4.1.274
HYL-1
ASAH-1
CGT-2
ASM-3
Glucosylceramide
Ceramide
Sphingomyelin
GBA-4
SMS-2
TTM-5
Dihydroceramide
c
Ground Control (GC)
Simulated Microgravity (MG)
Ceramides (ng/mL)
1500
1000
500
0
C14
C16:1
C16
C18:1
C18
C20
C22
C24:1
C24
C26:1
C26
Species
b
d18:1 Sphingosine (ng/mL)
55
50
45
40
35
GC
MG
Total Ceramide (ng/mL)
5000
4500
4000
3500
Total HexCer (ng/mL)
1600
1200
800
Total LacCer (ng/mL)
2000
1500
1000
500
0
Total SB (ng/mL)
100
75
50

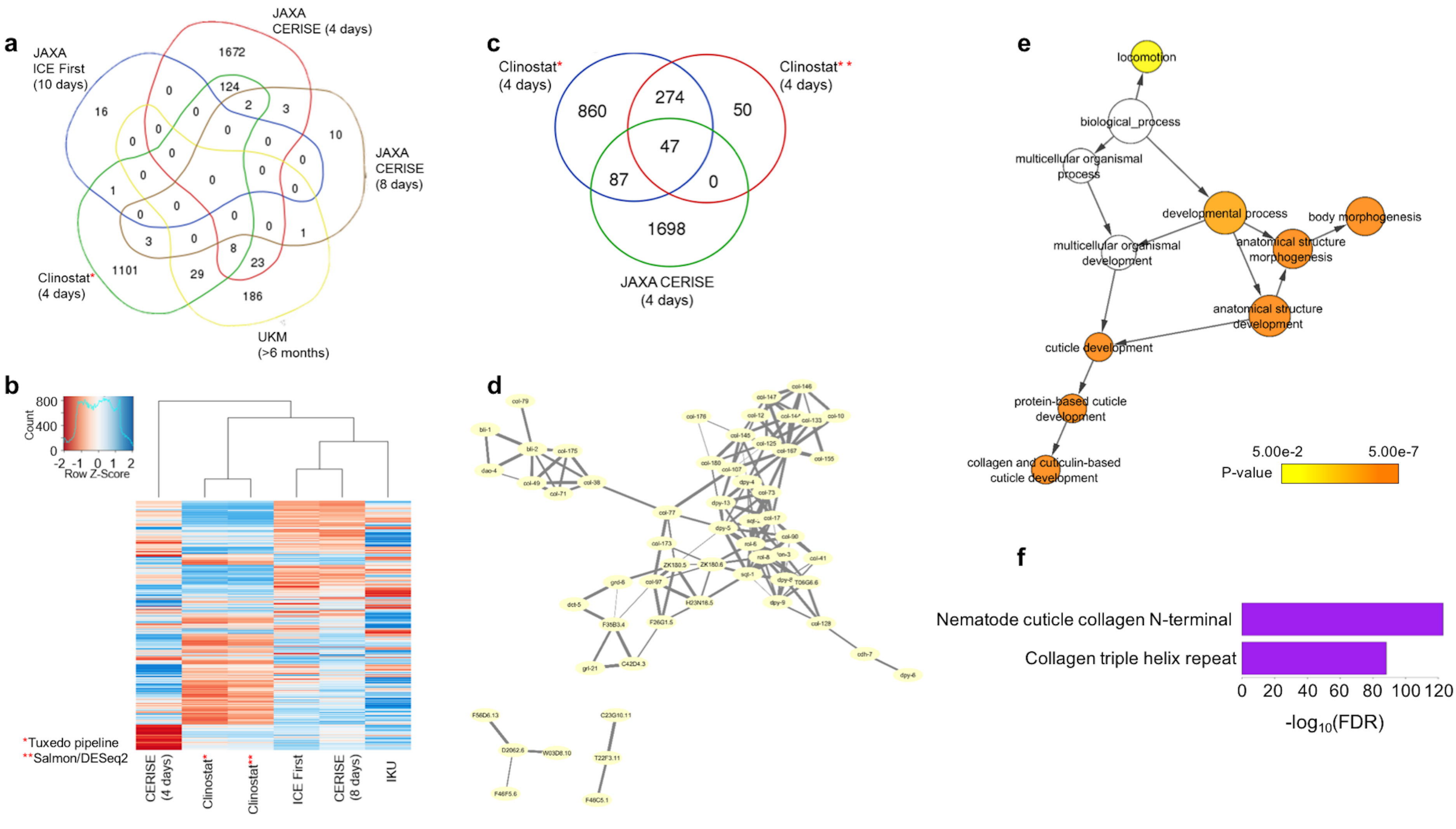
a
JAXA
CERISE (4 days)
JAXA
ICE First
(10 days)
JAXA
CERISE
(8 days)
Clinostat*
(4 days)
UKM
(>6 months)
1672
124
16
10
1101
29
186
23
b
Count
800
400
0
-2 -1 0 1 2
Row Z-Score
*Tuxedo pipeline
**Salmon/DESeq2
CERISE (4 days)
Clinostat*
Clinostat**
ICE First
CERISE (8 days)
IKU
c
Clinostat*
(4 days)
Clinostat**
(4 days)
860
274
50
47
87
0
1698
JAXA CERISE
(4 days)
d
e
locomotion
biological_process
multicellular organismal process
developmental process
body morphogenesis
multicellular organismal development
anatomical structure morphogenesis
anatomical structure development
cuticle development
protein-based cuticle development
collagen and cuticulin-based cuticle development
5.00e-2
5.00e-7
P-value
f
Nematode cuticle collagen N-terminal
Collagen triple helix repeat
0 20 40 60 80 100 120
-log10(FDR)